CHAPTER 4

Methods for determining the states of an artillery gun under dynamic disturbances

Oksana Maksymova
Pavlo Gultsov
Volodymyr Demydenko
Yevhenii Dobrynin

Abstract

This chapter develops a comprehensive model for assessing the technical condition and combat capabilities of a self-propelled artillery system (SPAS) considered as a complex dynamic object operating under conditions of cumulative wear and exposure to external combat factors. An approach to formalizing the system state is proposed, based on the integration of acoustic, visual, thermodynamic, and mechanical parameters with the construction of a generalized system of serviceability criteria.

Mathematical models are developed to describe the acoustic field of a shot, the processes of formation and evolution of the muzzle discharge, as well as methods for evaluating barrel stability with account taken of thermal and mechanical wear factors. An information model of artillery barrel operation is formulated, incorporating multivector serviceability conditions and enabling automation of residual life calculations.

A state tree of the system is constructed for rank-based assessment of the current technical condition, and combat capability criteria are integrated into a unified decision-making model using the ideal point method. An analytical relationship is derived to determine the required number of rounds to engage a target with a specified probability, together with a time-based model for evaluating mission execution that considers a window of particular vulnerability and maneuverability constraints. Computational examples demonstrate the practical implementation of the proposed approach and its applicability to assessing the risk of system loss and substantiating the advisability of opening fire.

The results establish a methodological foundation for further automation of condition monitoring of artillery systems and may be employed as an algorithmic module within decision-support systems for combat employment.

 DOI: 10.21303/978-9908-8450-1-2.ch4

Keywords
Self-propelled artillery system, dynamic assessment, combat capability, barrel service life, state tree, decision-making model, time budget.

4.1 Introduction

Modern artillery systems operate in highly dynamic conditions characterized by rapid fire exchange, intensive mechanical and thermal loading, and the necessity for continuous assessment of technical state and combat readiness. Under such conditions, traditional static evaluation approaches are insufficient, and operational monitoring based on physical signals generated during firing becomes essential.

Acoustic emissions, thermal radiation of muzzle gases, mechanical vibrations, and optical manifestations of the muzzle blast contain informative data about internal ballistic processes and system condition. Processing such heterogeneous information requires mathematical models combining physical description with statistical estimation and parameter identification techniques [1–3].

Existing studies have addressed individual aspects of artillery system assessment, including acoustic monitoring of firing processes, thermal diagnostics of barrel condition, and statistical models for projectile trajectory estimation. In many of these works, attention is primarily focused on the analysis of specific physical signals or on isolated parameters characterizing firing efficiency and barrel wear. While such approaches provide valuable diagnostic information, they are typically limited to separate subsystems or measurement modalities and do not explicitly integrate operational factors such as ammunition availability, mobility constraints, and survivability considerations. In contrast, the approach proposed in this chapter aims to combine heterogeneous physical indicators with operational parameters within a unified dynamic framework for evaluating the current combat capability of a self-propelled artillery system.

Repeated thermal and mechanical loading leads to barrel wear, erosion, and structural degradation, which affect projectile velocity and firing accuracy. Therefore, predictive models for resource estimation based on operational data are required to evaluate residual service life and system performance [4–6].

Modern combat doctrine emphasizes high-mobility tactics such as "shoot-and-scoot", where fire missions are followed by immediate relocation to reduce vulnerability. Decision-making must account for technical parameters, ammunition availability, mobility constraints, and survivability. Formalized state models and transition-based representations provide a unified framework for integrating these factors [7–9].

This chapter develops a system of dynamic criteria for evaluating the current combat capability of a SPAS. The criteria include firing efficiency, accuracy degradation, ammunition stock, mobility level, and ability to operate under partial system damage. Their aggregation into an integrated metric enables quantitative comparison of operational states and supports tactical decision-making.

Special attention is given to engagement scenarios involving high-value time-critical targets. In such situations, feasibility analysis must consider probabilistic hit models, time constraints, and survivability risks. The proposed framework integrates resource assessment, mobility analysis, and probabilistic engagement modeling into a coherent structure suitable for practical implementation in automated support systems [10].

The methodological approach is illustrated using parameters typical for modern 155-mm self-propelled artillery systems, with the Archer SPAS (BAE Systems, Sweden) used as a representative prototype for numerical modeling.

4.2 Analysis of models and methods for determining the states of an artillery gun

Mobility of artillery is a determining factor in preserving combat capability, since counter-battery warfare systems enable the adversary to rapidly detect firing positions and deliver a retaliatory strike. This has led to the widespread adoption of the "shoot-and-scoot" tactic, which involves executing a fire mission followed by an immediate change of position. Modern artillery systems, due to their high rate of fire and mobility, implement multiple cycles of "shot – displacement – shot" within a short time interval [11].

Scientific sources consider models that account for rate of fire, targeting procedures, firing errors, and the probability of target engagement, as well as approaches to selecting positions and routes with regard to terrain topology and feedback control [12]. The Markov model of artillery combat describes the organization of fire but does not account for the reduction in effectiveness caused by combat damage during maneuvering. Studies [13, 14] emphasize temporal parameters of combat and the minimization of target engagement time while considering the risk of detection after the first shot.

For the analysis of the artillery system state, informational features of a shot are considered (**Fig. 4.1**). The main features include the acoustic fields of the ballistic and muzzle waves (MW), as well as visual manifestations of the muzzle discharge in the visible and infrared spectra. Assessment of system operability additionally accounts for barrel wear, deterioration of the running gear, and possible combat damage.

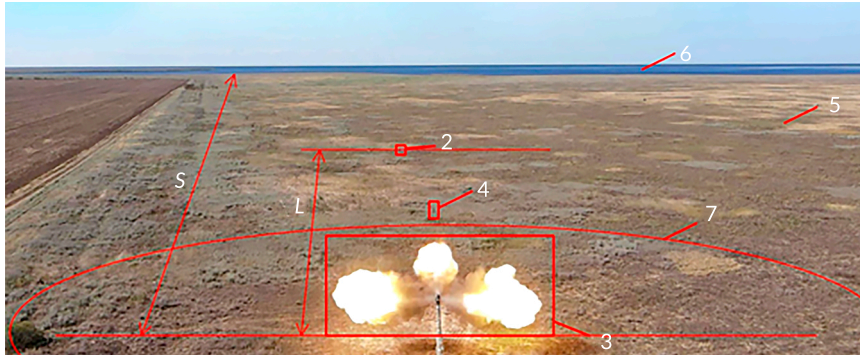

Fig. 4.1 Situational layout of the artillery system: 1 – gun; 2 – measuring system; 3 – propellant gases forming a shock-acoustic wave; 4 – projectile on a ballistic trajectory; 5 – mainland surface of the training ground; 6 – sea surface of the training ground; 7 – boundary of transition from the shock MW to the acoustic MW; *S* – distance from the firing position to the target; *L* – distance from the firing position to the location of the measuring system

4.3 Acoustic waves for the identification of artillery guns

Acoustic field of a shot is formed by ballistic and muzzle waves and can be used to determine the location of an artillery system [15]. Physical models and experimental data make it possible to establish the main parameters of these waves and assess their informational value.

When a projectile flies at a velocity $V > c$, a ballistic wave (BW) is formed with a front in the form of a Mach cone. The opening angle is determined by

$$Q_M = \arcsin(1/M), M > 1, \tag{4.1}$$

where M – the Mach number.

The BW signal is a short-duration broadband pulse lasting 3–8 ms with a characteristic frequency band of 1–10 kHz. Its amplitude and temporal parameters can be estimated using the empirical acoustic model of a shock wave generated by a supersonic projectile (Whitman model), which is applied in studies devoted to estimating flight parameters based on acoustic signals:

$$A = \frac{0.53P_0(M^2-1)^{1/8}\varphi}{d_{sM}^{3/4}l^{3/4}}, \tag{4.2}$$

$$T_N \approx \frac{1.82\varphi}{c}\left(\frac{M\varphi}{l}\right)^{1/4}, \tag{4.3}$$

while the rise (and decay) time of the pulse front is

$$t_r = t_d \approx \frac{\lambda}{c}\frac{P_0}{A},$$

where A – the amplitude of the BW, Pa; T_N – the duration of the main part of the pulse; $t_r \approx t_d$ – the duration of the rise and decay fronts of the BW pulse, respectively; P_0 – the atmospheric pressure; φ – the projectile caliber; l – the projectile length; d_{sM} – the shortest distance from the recording point to the Mach cone; c – the speed of sound in air; $\lambda \approx 6.8 \times 10^{-8}$ m – the mean free path of an air molecule.

The BW is recorded by a microphone only if the observation point lies inside the Mach cone. At a certain point along the trajectory, the projectile velocity becomes lower than the speed of sound, and the wave disappears; therefore, it must be recorded at relatively short distances from the firing point. Due to the short rise time of the BW, it must be recorded with a high sampling rate.

The MW is formed as a result of the expansion of propellant gases after the projectile exits the barrel. It propagates at the speed of sound and has an impulsive character with a sound pressure level of up to 150 dB. The signal duration is 30–50 ms, and the main spectral range extends up to 100 Hz.

The shape of the overpressure pulse can be described by the generalized Friedlander model

$$P_{mw} = A_{mw}\left(1 - \frac{t}{T_0}\right)e^{-\beta t/T_0}, \tag{4.4}$$

where A_{mw} – the pulse amplitude; T_0 and β – parameters defining the pulse shape.

Alternatively, the Berlage model is applied to describe the oscillatory structure of the pulse tail

$$P_{mw}^{B} = A_{mw}t^{nr}e^{-\alpha t}\sin(2\pi f_0 t), \tag{4.5}$$

where nr – the exponent characterizing the power-law rise rate of the leading front of the MW; α – the attenuation coefficient of the oscillatory process of the MW; f_0 – the dominant frequency.

The MW front has a spherical character; however, at distances exceeding 50 m it may be considered planar. For ranges up to 2–3 km, the amplitude of the muzzle wave typically exceeds that of the ballistic wave by a factor of 2–3 [15].

Within the structure of the acoustic signal, the ballistic wave is recorded earlier than the MW, since $V > c$. After the short ballistic wave impulse, a pause is observed, followed – after a temporal delay – by the arrival of the muzzle wave. The total duration of recording the signal of a single shot is approximately 0.6 s.

When recording signals in the near-ground atmospheric layer, the dominant interference is wind noise, which spectral density decreases proportionally to $1/f$, corresponding to the "pink noise" model. Experimental data confirm the adequacy of such a description.

A typical representation of the recorded acoustic field at SNR = 10 dB is shown in **Fig. 4.2**. The segments corresponding to the ballistic wave and the muzzle wave are clearly identified in the recording against the noise background. Analysis of experimental data confirms the adequacy of the pink noise model for describing real interference.

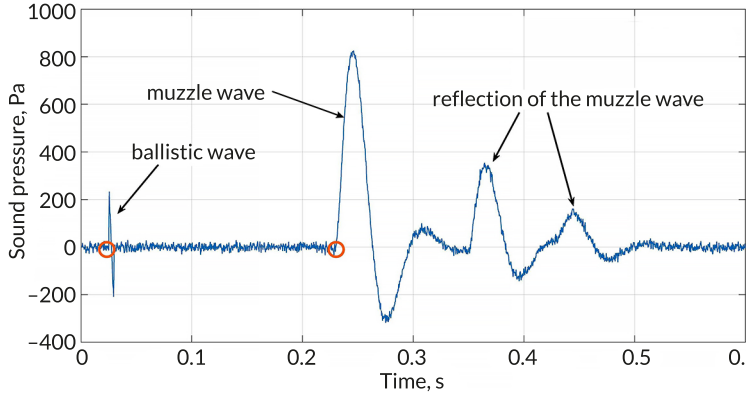

Fig. 4.2 Typical view of the recorded acoustic field

4.4 Visual field of propellant gases in the muzzle discharge

The muzzle discharge of propellant gases after the projectile exits the barrel exhibits a complex spatial structure formed by the axial flow and lateral jets through the openings of the muzzle brake. The dynamics of its development contain informative features for the identification of the artillery system. Their registration is possible by means of high-speed video recording. Experimental data from field firing tests were used for the analysis [16].

Studies [17, 18] substantiate the feasibility of using video data of the muzzle discharge for diagnosing the state of an artillery system. Temporal changes in the geometric parameters and temperature of the gases during the transition from a shock wave to an acoustic wave have been recorded.

Fig. 4.3 presents a generalized frame-by-frame sequence of the development of the muzzle discharge for different variants of propellant charges at characteristic time moments of 0.04 s and 0.12 s after the projectile exits the barrel. The selected intervals correspond to the initial stage of gas volume formation and the stage of its intensive expansion. A comparison of the frames indicates significant differences in the spatial configuration and luminosity intensity for charges with different energy characteristics.

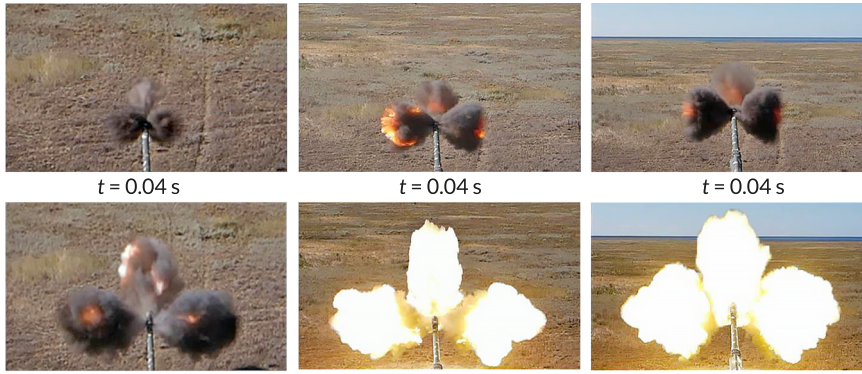

Fig. 4.3 Development of the muzzle discharge for different variants of propellant charges at characteristic time moments: *a* – shot with minimum propellant charge; *b* – shot with full propellant charge; *c* – shot with the first propellant charge

The complete temporal evolution of the process within the interval of 0.04–0.16 s is presented in **Table 4.1**. Joint data processing revealed differences in the projected pressure and temperature distributions for different charges. The transition time from the shock wave to the acoustic wave depends on the charge energy and lies within 0.04–0.12 s after projectile exit.

Geometric and temperature parameters of the muzzle discharge can be used as identification features of a shot.

The time interval from 0 to 0.20 s is characterized by intensive formation and expansion of the muzzle discharge volume, which is analyzed in detail for

different charge variants (**Fig. 4.3**, **Table 4.1**). Further development of the process is mainly determined by the interaction between the gas volume and the atmospheric environment.

Table 4.1 Perimeter of the generatrix, projected area, and gas temperature in the muzzle discharge within the time interval of 0.16 s after projectile exit

Time, s	Minimum charge			Full charge			First charge		
	Perimeter, m	Area, m^2	Temperature, K	Perimeter, m	Area, m^2	Temperature, K	Perimeter, m	Area, m^2	Temperature, K
0.04	10.17	3.76	1020	16.14	9.21	1420	19.12	11.45	1390
0.08	17.77	10.52	910	25.97	16.97	1330	25.88	21.6	1290
0.12	22.72	16.46	950	33.64	26.85	1250	34.77	33.94	1200
0.16	64.72	23.99	1180	39.35	25.4	1100	40.84	41.74	1050

The analysis results make it possible to distinguish two independent identification channels. The first is the variation of the projected area of the muzzle discharge volume, which increases monotonically until pressure equalizes with the atmosphere, after which its evolution is governed by diffusion and wind-driven processes [18, 19]. The dynamics of this process are observed within the time interval of 0–0.2 s and are characterized by a stable tendency toward an increase in the projected area.

The second is the temperature characteristic of the gas volume, which decreases during expansion but may exhibit a local maximum at the moment of oxidation of combustion products in the atmosphere. The mixing of propellant gases with atmospheric oxygen is accompanied by oxidation of soot particles and additional energy release, which explains the possible temperature surge and the appearance of a flame.

Within the time interval up to 0.20 s, a characteristic spatiotemporal structure of the muzzle discharge is formed, after which the process transitions to a stage of gradual reconfiguration and interaction with the atmospheric environment.

Fig. 4.4 illustrates the development of the three-lobed shape of the muzzle discharge within the interval of 0.24–0.54 s after the shot. The frame sequence is presented with a time step of $\Delta t = 0.08$ s. Visual features of the shot persist for up to 1 s after the projectile exits the barrel.

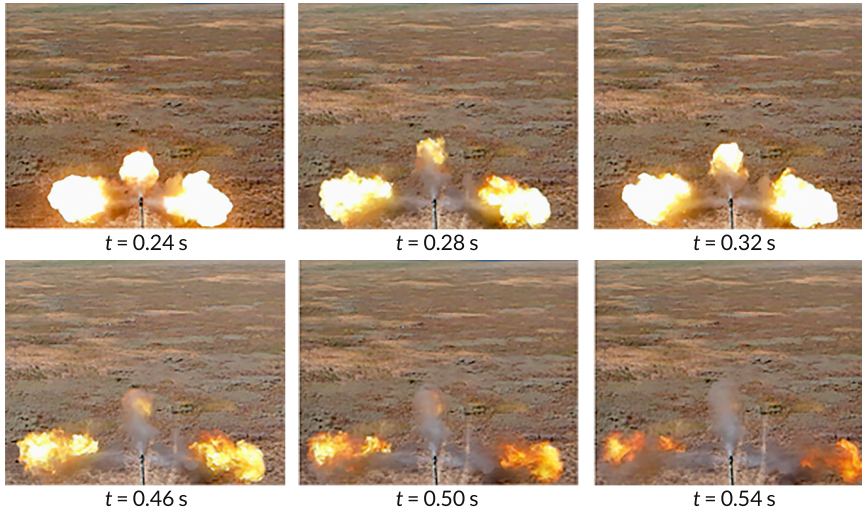

Fig. 4.4 Demonstration of the three-lobed muzzle discharge of the artillery system as a function of time after the shot

4.5 Methods for calculating the stability of artillery system barrels

4.5.1 Methods and models for calculating the stability of an artillery barrel

Barrel stability (service life) is determined by the wear rate of the bore and depends on two groups of factors – thermal and mechanical.

Thermal factors include:

– heating of the bore by propellant gases with temperatures of 2000–3500 K;

– heating of the bore surface due to frictional heat in the contact zone of the projectile driving bands;

– heat generation within the barrel metal caused by deformation under the pressure of propellant gases and the impact interaction of the projectile's centering band with the rifling.

Mechanical factors are associated with wear of the heated barrel resulting from erosive removal of metal by the flow of propellant gases, as well as wear in the clearances between the projectile driving band and the bore surface and its guiding elements.

The wear intensity is determined by the gas temperature, the projectile muzzle velocity, the barrel caliber, and the material properties. The permissible number of shots N is estimated using the empirical relationship

$$N = \frac{K_T}{C_q^3 v_0^{4.5} d^{2.5}}, \tag{4.6}$$

where K_T – the temperature coefficient accounting for the energy capacity of the propellant and the characteristics of the barrel steel; C_q – the weapon power; v_0 – the projectile muzzle velocity; d – the bore diameter.

For guns with similar ballistics and a constant propellant grade, K_T is assumed to be constant.

If the value of the coefficient K_T is unknown, expression (4.6) is conveniently used for a comparative assessment of stability when varying the muzzle velocity, caliber, and projectile mass. As a first approximation, K_T may be taken for medium-caliber guns as $K_T \approx 7 \times 10^{24}$. It is important to correctly determine stability for high-power systems characterized by $Cq = mv_0^2 / 2d^3 \approx 400$ tf · m/dm^3.

The firing mode significantly affects barrel heating and, consequently, its service life. At high rates of fire, critical deformations and a reduction in accuracy are possible; therefore, stability control is ensured by limiting burst length and intervals between shots.

For calculating the stability of such systems, Yustrov's expression may be applied

$$N = \frac{xy}{d^2} \frac{C_q v_0^2 \sigma \varepsilon}{\lambda \mu k_1}, \tag{4.7}$$

where $x = f_1(p_{max}, R, k, Q_h)$; p_{max} – the maximum pressure in the barrel bore; R – the gas constant of the propellant gases; k – the adiabatic exponent of the propellant gases; $y = f_2(d, n)$; n – the rate of fire; $\lambda = L_c / d$, where L_c – the barrel length; σ – the ultimate tensile strength of the barrel material; ε – the relative tangential strain of the barrel walls; μ – the friction coefficient of the driving band against the barrel walls; k_1 – the compressive strength of the driving band material; C_q – has the dimension of gf/cm^3; d – has the dimension of cm. Barrel stability N is determined by a 10% reduction in the muzzle velocity v_0.

Various empirical relationships (Yustrov, Linthe, Gabo, Slukhotsky) are used to estimate service life, taking into account geometric, ballistic, and technological parameters. However, their applicability is limited to specific experimental conditions; therefore, modern systems require adaptation of the models based on actual operational data.

4.5.2 Methods and models for calculating the stability of the "barrel – charge – projectile" system

Methods and models of wear and stability are considered as a consequence of the transition from lumped to distributed system properties. This approach is necessary for predicting barrel stability without conducting experimental testing and for evaluating the effectiveness of technological measures aimed at reducing wear. Mathematical models must take into account the characteristics of the "barrel – charge – projectile" system and the effectiveness of the applied technologies.

The complexity of modeling is determined by the large number of factors influencing wear and stability. A simulation model should include the calculation of the barrel temperature field, bore wear characteristics, internal ballistic parameters of the shot, projectile dispersion for a worn barrel, and the functional limit of the projectile driving elements.

In calculation methods, reliance on "analogs" creates the problem of the absence of reference values. Therefore, modern computational approaches employ fundamental mathematical models with a high level of generalization rather than empirical formulas based on lumped properties. Thermal field modeling is performed under firing regimes typical for the barrel and involves the selection of "analogues" based on heat transfer and wear results.

The specific diametral wear Δd_{spec} is calculated per shot, taking into account the geometry of the bore, the firing regime, instantaneous heat transfer and cooling coefficients, as well as the thermophysical properties of the material. The maximum surface temperature of the bore T_l^m is determined for a series of cross-sections. Based on this value, the material damage characteristic of the bore δ_d and the corresponding energy expenditures for damage formation A_d are determined.

The empirical dependence of the specific diametral wear can be expressed as a power function

$$\Delta d = A(T_l^m)^{\alpha}(\delta_d)^{\beta}(A_d)^{\gamma}, \tag{4.11}$$

where A – the experimental coefficient; α, β, γ – experimentally determined exponents.

The values of the arguments and the coefficient A are determined on the basis of design – ballistic and operational data, taking into account the adopted calculation method. The application of the dependence to new weapon systems is valid within the limits of parametric similarity to the reference "analogue" for which its identification was performed.

Based on Δd, the following barrel bore parameters are calculated: the elongation of the chamber $\Delta\lambda_1$, the increase in projectile travel distance until complete engagement of the driving band $\Delta\lambda_2$, and the area of propellant gas breakthrough δS. Neglecting the longitudinal wear δl and approximating the wear curve by a straight line, let's obtain:

$$\Delta\lambda_1 = 0.5d\,\mathrm{ctg}\beta\left(1-\frac{D_0-d}{\Delta d}\right),$$
$$\Delta\lambda_2 = 0.5d\,\mathrm{ctg}\beta,$$
$$\delta S = 0.5\pi d\Delta d\left(1-\frac{D_0-d}{\Delta d}\right). \qquad (4.12)$$

These dependencies are valid under the condition that $(D_0-d)/\Delta d<1$.

Otherwise, $\Delta\lambda_1 = 0$, $\delta S = 0$, and only the geometry of the forcing cone changes.

The value of cot β is corrected based on experimental data. The calculation is performed for the extreme values of the expected number of shots (N_1, N_2) or for a single number of shots N.

To assess the internal ballistic characteristics of the shot and the reduction in muzzle velocity, the internal ballistic problem for a worn barrel is solved, taking into account the engagement of the driving band and gas leakage. The failure criterion of the driving elements is determined simultaneously. Methods of plasticity theory account for the dynamic deformation of the driving band (DB) and make it possible to determine whether the protrusions of the DB will be sheared and whether the barrel will reach its stability limit at a given level of wear.

Barrel stability is assessed by comparing the reduction in muzzle velocity Δv_0 and the shear of the driving band. This can be performed for a given N or for an admissible velocity reduction Δv_0^{perm} at which the corresponding $\Delta\lambda_1$, $\Delta\lambda_2$, and δS are determined.

To evaluate stability according to the criterion of projectile dispersion or ovality of impact holes, the external ballistic problem is solved, taking into account the initial deviations of translational, rotational, and nutation velocities caused by bore wear.

4.6 Information modeling of artillery barrel operation

The task of modeling the operation of an artillery barrel is associated with incomplete or redundant and potentially contradictory input data. This specificity necessitates a stepwise consideration of the process, taking into account the intensity of combat operations.

4.6.1 Automation of modeling of artillery barrel operation

Automation must ensure the input of any initial data obtained during operation, as well as monitoring of the limiting properties of the barrel required for mission execution.

The result of modeling artillery barrel operation is the acquisition of reliable data on the service life and the characteristics of its variation depending on the initial firing conditions. The system must provide the possibility, at the operator's discretion, to use non-limit values of the input data to extend the period of resource utilization without violating the logic of combat operations.

The formation of different scenarios for the use of residual service life is envisaged.

The informational nature of the process makes it possible not only to automate modeling but also to optimize it in real time on the basis of modern computing systems. The information model is considered as a set of mathematical models of distributed properties, models of serviceability states, and interface tools for displaying results. The basis for constructing the information model is the need to assess the barrel state, ensured by a set of model-based calculations of its current properties. The sources for model formation include technical documentation of the weapon system, results of range and ballistics tests, as well as statistical data from serial production.

The model input data include constants of mechanical, thermophysical, and chemical-kinetic quantities, as well as data arrays of properties required for calculations.

The analysis of the processes occurring in the barrel during operation has made it possible to identify groups of parameters for evaluating the residual service life.

The first group characterizes the general, longitudinal, and local strength of the barrel. The serviceability condition for this group has the form $\sigma \le [\sigma]$ and $P_1 \le [P]$, where $\sigma = \{\sigma_{eq}, \sigma_{ej}, \sigma_{mb}\}$ – the vector of calculated strength parameters; $P_1 = \{p_1^{el}, p_1^{scr}, p_2^{sh}, p_{\text{lim}}, p_{fail}\}$ – the vector of calculated allowable elastic and resistance parameters; $[\sigma]$ – the vector of allowable stress values; $[P]$ – the vector of required resistance values; the corresponding safety factors are determined experimentally; σ_{eq} – the equivalent stress in the barrel rifling; σ_{ej} – the maximum stress in the region of injection holes; σ_{mb} – the maximum stress before the muzzle thickening; p_1^{el} – the elastic limit of the monoblock; p_1^{scr} – the limit of possible resistance of the reinforced (banded) barrel; p_2^{sh} – the elastic resistance of the barrel sleeve; p_{lim} – the conditional elastic limit; p_{fail} – the destructive pressure.

The second group characterizes changes in the shape, dimensions, and surface condition of the bore and is defined by the condition $\delta \le [\delta]$. The components of the vector describe the state of the bore with respect to wear and may be determined either analytically or experimentally: $\{\Delta d_{wps}, \Delta\lambda_{ch}, \delta_m, \delta_{st}, \delta_{pl}, \delta_T, l_{cr}\}$ where Δd_{wps} – the

diametral wear per shot; $\Delta\lambda_{ch}$ – the chamber elongation; δ_m – the depth of the melting zone; δ_{st} – the depth of the structural transformation zone; δ_{pl} – the depth of the plastic deformation zone; δ_T – the thermal expansion of the bore; l_{cr} – the average crack length.

The third group describes the barrel as a mechanical vibrational system and is defined by the condition $\gamma \le [\gamma]$, where the vector components are $\gamma = \{\gamma_m, f_{st}, EI, v_i\}$, γ_m – the muzzle angle; f_{st} – the static deflection of the barrel under its own weight; EI – the bending stiffness of the barrel; v_i – the natural frequencies corresponding to radial, transverse, and longitudinal vibration modes.

The fourth group characterizes the barrel as a structural element of the system and is defined by the condition $\varepsilon \le [\varepsilon]$, where the vector components are $\varepsilon = \{Q_b, J_i, x_{cm}, \delta r_j, T_{ch}, P_b\}$ where Q_b – the barrel mass; J_i (i = 1, 2) – the mass moments of inertia; x_{cm} – the coordinate of the center of mass; δr_j – the radial expansion of the barrel at the junction with the cradle; T_{ch} – the chamber surface temperature; P_b – the force acting on the breech.

The thermal factor affects all groups of parameters and determines changes in the permissible stress values and material properties. This influence extends both to the magnitude of the parameter on the left-hand side of the inequality and to the magnitude within the allowable limit.

Non-uniform heating of the barrel wall leads to the development of thermal stresses and to a reduction in the allowable stress due to the degradation of the strength properties of structural steel at elevated temperatures.

The maximum surface temperature of the barrel is a determining factor in wear and must be taken into account within the second group.

For different groups of barrel parameters associated with possible failure during operation, different characteristics of the thermal field are significant.

For the parameters of the first group, the temperature gradient and the overall heating level are important; for the second group, the maximum temperatures are significant; for the third group, the longitudinal temperature gradient is decisive; and for the fourth group, the integral thermal characteristic δr_j is relevant.

Therefore, the thermal aspect of the serviceability conditions is expressed by the inequality $T \le [T]$, where the vector of characteristic thermal parameters is $T = \{T_{b0}, T_{\max}, T_{ch0}, \Delta T_L, T_{p(x)}, T_{cool}, T_{avg(r)}\}$ where T_{b0} – the bore surface temperature at the beginning of rifling before the current shot, characterizing the overall heating level; $T_{\max}$ – the maximum bore surface temperature; T_{ch0} – the chamber surface temperature before cartridge insertion; ΔT_L – the longitudinal temperature difference of the average wall temperature along the barrel; $T_{p(x)}$ – the temperature profile at the cross-section corresponding to the maximum pressure; T_{cool} – the coolant

temperature at the outlet of the continuous cooling system; $T_{avg(r)}$ – the average temperature across the wall thickness.

Each of the listed property vectors should be understood as open, since the development of concepts regarding barrel serviceability expands the set of parameters. The system of inequalities forms a generalized model of the serviceability conditions. Its practical implementation requires the accumulation and systematization of experimental data, followed by iterative verification for new weapon systems.

4.6.2 Automation of calculations using internal ballistic models for assessing barrel condition and service life

Modern computational tools make it possible to automate the solution of internal ballistics problems and the assessment of barrel stability parameters, including the modeling of gas-dynamic processes, optimization problems, and inverse calculations.

Classical approaches include empirical, analytical, and hybrid methods for solving the main internal ballistic problem, in particular models based on the generalized thermodynamic scheme of STANAG 4367.

4.7 Method for dynamic assessment of the current combat capability of an individual self-propelled artillery system

4.7.1 System of criteria for dynamic assessment of combat capability

Let's consider a new combat unit – a next-generation SPAS. As a prototype, the Archer SPAS manufactured by BAE Systems (Sweden) [20] is selected, and its tactical and technical characteristics are adopted as the baseline for subsequent modeling.

Let's assume that the general scheme of combat employment of an individual SPAS has the following structure. During targeting, i.e., determining the priority of targets and the sequence of their engagement [21], the system is assigned N targets T_i by the higher-level command, and their coordinates $(x_i^T, y_i^T), i = 1,...,N$, are communicated for sequential engagement.

Target engagement is carried out from prepared firing positions $FP_i, i = 1,...,N$, each of which lies within the firing range corresponding to the respective target. After firing at target T_i from position i, and in accordance with the "shoot-and-scoot" concept, the SPAS moves to position $I + 1$ to engage target (**Fig. 4.5**).

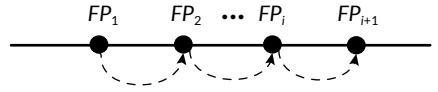

Fig. 4.5 Scheme of movement of the SPAS according to the "shoot-and-scoot" concept

Since combat capability can be assessed using different indicators, the following criteria were selected:

1. Current shot effectiveness. Shot effectiveness is determined by relation (4.13) according to [1]. This implies that the projectile muzzle velocity, reduced due to barrel wear, $(v_0^{table} - \Delta v_0^t)/v_0^{table}$, at the moment of assessment t is at least 0.95 of the tabulated value v_0^{table}. In the proposed methodology, the level of correct assessment of current shot effectiveness is determined using a rank-based control criterion:

$$Crit_1 = (v_0^{table} - \Delta v_0^t)/v_0^{table}, \tag{4.13}$$

$$Crit_1 = \begin{cases} 1, n_{shot}^t \le 25; \\ 1/2, 25 < n_{shot}^t \le 40; \\ 1/3, n_{shot}^t > 40, \end{cases} \tag{4.14}$$

where Δv_0^t – the deviation of the muzzle velocity from the tabulated value; n_{shot}^t – the number of shots fired from the barrel from the time of the last instrumental assessment of the muzzle velocity v_0 up to the moment of firing t.

The acceptance criterion is defined by the condition $Crit_1 \ge 0.95$.

2. Shooting accuracy reduction factor. This criterion accounts for combat damage (indirect hits) inflicted on the SPAS by the adversary, $n_{attacks}$. Such damage reduces the probability of a shot hitting the target p_{fact} compared with the probability of hitting without damage p:

$$Crit_2 = p_{fact}/p, \tag{4.15}$$

$$Crit_2 = \begin{cases} 1, n_{attacs} = 0, \\ 1/2, n_{attacs} = 1, \\ 1/3, n_{attacs} = 2. \end{cases} \tag{4.16}$$

3. Residual ammunition stock (ammunition stock). The assessment of the residual ammunition stock at time t, AS_t, is performed according to the criterion

$$Crit_3 = AS_t = (AS_{full} - n_{shots}^t)/AS_{full}, \tag{4.17}$$

where AS_{full} – the full ammunition load of the SPAS. The critically low value of the criterion $Crit_3$ is considered to be $AS_t^* = 3$ (for $AS_{full} = 21$).

4. Capability of firing in MRSI mode. The ability to fire in MRSI (Multiple Rounds Simultaneous Impact) mode may become unavailable due to indirect enemy hits causing failure of the vertical barrel elevation mechanism or its control system. Accordingly, the capability of firing in MRSI mode is evaluated according to the criterion:

$$Crit_5 = \begin{cases} 1, n_{attacs} < 2, \\ 0, n_{attacs} \geq 2. \end{cases} \tag{4.18}$$

The value 1 indicates the possibility of operating in MRSI mode, while 0 denotes its loss as a result of damage to the vertical elevation mechanism or its control system when $n_{attacs} \geq 2$.

5. Rate of fire. The rate of fire of the SPAS may decrease due to indirect enemy projectile hits. The current rate of fire RF_t is proposed to be evaluated according to the following criterion:

$$Crit_4 = \begin{cases} 1, level = 1, \\ 1/2, level = 2, \\ 1/3, level = 3. \end{cases} \tag{4.19}$$

The first level of rate of fire corresponds to the situation $RF_t = RF_{\max}$ shots per minute, where $RF_{\max}$ is the maximum rate of fire; the second level of rate of fire corresponds to the condition $RF_t = RF_{\max} - 2$; the third level of rate of fire corresponds to the condition $RF_t = RF_{\max} - 3$.

6. Residual mobility. The SPAS movement from one firing position to another may be carried out either via roads or across rough terrain. Despite the adaptability of next-generation systems to movement along complex off-road routes, the tires of wheeled chassis may be damaged during such movement, resulting in a temporary reduction in speed and a decrease in mobility. The residual mobility at time t is proposed to be evaluated according to the criterion:

$$Crit_6 = \begin{cases} 1, level = 1, \\ 1/2, level = 2, \\ 1/3, level = 3. \end{cases} \tag{4.20}$$

Let v_t denote the average speed of movement of the SPAS over the time interval t. In this case, mobility corresponds to the first level if $v_t = v_{\max}$, where $v_{\max}$ – the

maximum movement speed; to the second level if $v_t = v_{max} / 2$; and to the third level if $v_t = v_{max} / 3$.

The six proposed criteria can be integrated into a unified assessment of the current combat capability of the SPAS using an aggregation based on the ideal point method with the L_2 norm

$$Crit_t^{ideal\_point} = \sqrt{\sum_{k=1}^{6} w_k (Crit_k - Crit_k^{ideal\_point})^2}, \quad \sum_{k=1}^{6} w_k = 1, \tag{4.21}$$

where $Crit_t^{ideal\_point}$ – the maximum possible value of the corresponding criterion; w_k – the weight of the respective criterion determined in accordance with the combat situation.

The proposed approach provides an integrated assessment of the current system state based on criteria (4.13)–(4.20).

4.7.2 Selection of the movement route between firing positions

It should be emphasized that the movement of the SPAS between firing positions may be carried out either along roads or across rough terrain, as shown in **Fig. 4.6**.

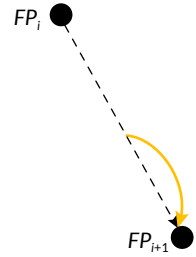

Fig. 4.6 Movement of the SPAS from position FP_i to position FP_{i+1} (yellow – road, black – rough terrain)

When moving along roads, the high travel speed significantly reduces the relocation time. However, roadways are typically subject to intensive enemy fire. Therefore, there is a risk of the SPAS being hit during movement.

When moving across rough terrain, the system's speed is lower; at the same time, wear of the running gear increases, but the probability of being targeted by enemy fire decreases and the movement trajectory becomes shorter.

If several possible routes exist for movement from position FP_i to position FP_{i+1}, the optimal one can be selected by solving a two-criteria transportation problem with minimization of the objective functions – ravel time t and losses Q:

$$\begin{cases} F_{tr}^1 = \min t(FP_i \Rightarrow FP_{i+1}), i = 1,...,n; \\ F_{tr}^2 = \min Q(FP_i \Rightarrow FP_{i+1}). \end{cases} \quad (4.22)$$

In this case, losses are evaluated as the product of the probability of a hit and the cost of the SPAS. It is proposed to assume that the probability of a hit is proportional to the time spent moving along a road under enemy fire. The two-criteria transportation problem is reduced to a linear programming problem. Its solution time on a computer of average performance does not exceed 5 seconds.

4.7.3 Model of combat operations in an exceptional tactical situation

Let's consider the combat employment of the SPAS in an exceptional tactical situation. The main task is counter-battery warfare, within which the system, using the "shoot-and-scoot" tactic, sequentially engages N targets T_i, moving between firing positions FP_i, $i = 1, ..., N$.

Consider a situation in which, after engaging target T_i from position FP_i, information is received about the appearance of a high-value target (EDT – especial danger target) requiring immediate engagement. The EDT is not an artillery battery but has significantly higher combat value. It must be engaged within a "window of especial danger" (WED) Δt_{WED}. The EDT is considered destroyed provided that at least two hits occur with probability p^*.

After receiving targeting information, the SPAS makes a short stop and opens fire from a temporary firing position (TFP). The spatial and temporal schemes are shown in **Fig. 4.7**, **4.8**.

It is assumed that after completing firing at position FP_i, a dynamic assessment of the current combat capability of the SPAS is performed using the method formulated above.

Based on the conducted dynamic assessment, a state tree of the SPAS is formed (**Fig. 4.9**), reflecting the most probable variants of event development.

Before constructing the decision tree, it is assumed that the SPAS moves on prepared road surfaces and that its mobility is not restricted by external conditions. Under such assumptions, criterion $Crit_6$ is set equal to one and does not affect the structure of the state tree.

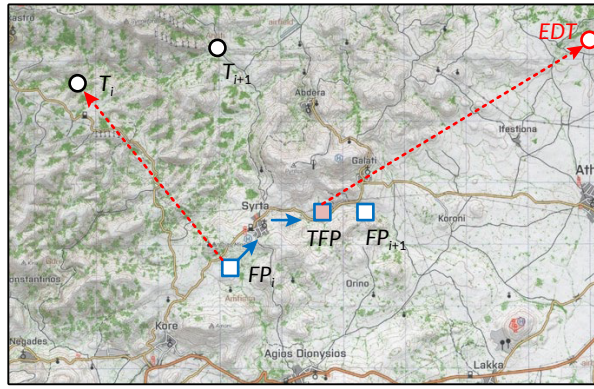

Fig. 4.7 Spatial scheme of firing at the EDT

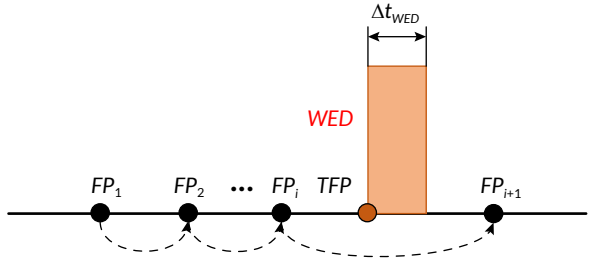

Fig. 4.8 Temporal scheme of firing at the EDT

The first branching level corresponds to criteria $Crit_1$ – $Crit_5$, while subsequent levels reflect the capability to perform combat operations and the rank-based assessment of parameters. The current state is represented by the tuple $State^t < 1,n1;\ 2,n2;\ 3,n3;\ 4,n4;\ 5,n5 >$, where $n1 \in \{1.1, 1.2, 1.3\}$, $n2 \in \{2.1, 2.2, 2.3\}$, $n3 \in \{3.1, 3.2\}$, $n4 \in \{4.1, 4.2\}$, $n5 \in \{5.1, 5.2, 5.3\}$ is the numbers of the terminal branches.

Further, the sequence for assessing the possibility of engaging the EDT is as follows.

Let the probability of a hit with a single shot in the ideal state be equal to p. Taking into account the current state, the adjusted value of p is determined in accordance with the state tree. Assuming independence of shots, the required number of shots n^* to ensure K hits with probability p^* is determined from the inequality

$$1-(1-p)^{n^*-K} \geq 1-p^* \geq (1-p)^{n^*-K}. \qquad (4.23)$$

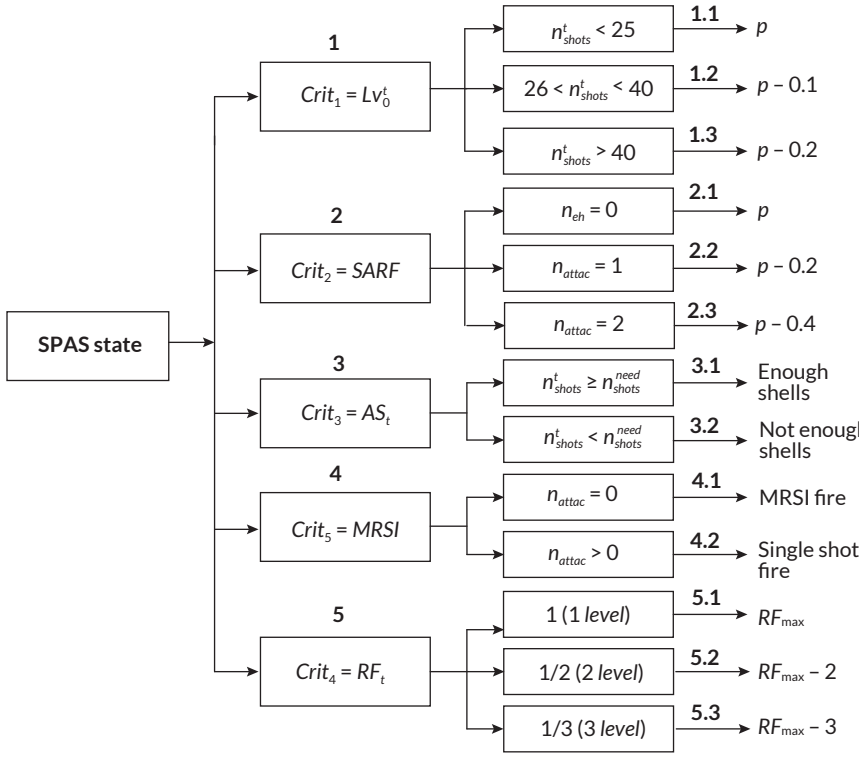

Fig. 4.9 State tree of the combat capability of the SPAS prior to the initial moment of engagement of the EDT

From this, the following relationship is obtained

$$n^* = \log(1-p^*)/\log(1-p) + K. \tag{4.24}$$

The formula is applicable for $0 < p < 1$.
After rounding

$$n^{**} = \lceil n^* \rceil \tag{4.25}$$

the number of shots required to destroy the target with probability p^* can be obtained. A visualization of relationship (4.24) is presented in **Fig. 4.10**.

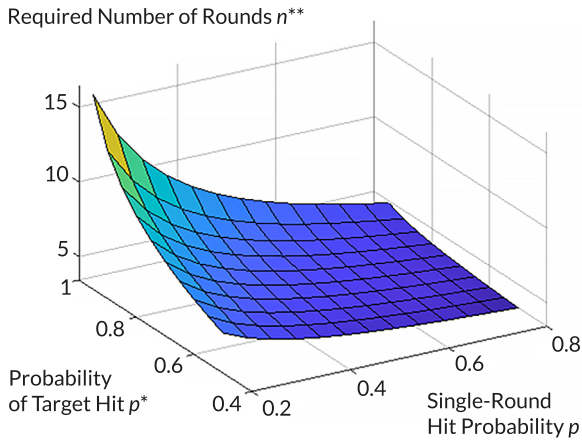

Fig. 4.10 Graphical representation of relationship (4.24)

Considering the discrete nature of the variable n^{**} (**Fig. 4.10**), only nodal values are used.

The obtained value n^* is correlated with the available ammunition load according to Criterion 3. If $n^{**} > (AS_{full} - n^t_{shot})$, the assigned task is infeasible. It is provided that the ammunition load is sufficient, the input data of Criterion 4 are verified. If firing in the MRSI mode is not possible, the operation can only be carried out by single shots with a rate of fire determined according to Criterion 5.

Subsequently, the time budget required to engage a high-priority target is assessed. The time allocated for accomplishing the fire mission against the EDT, denoted as t^*, includes the time required to prepare the artillery system for firing during a short halt t_{prep_fire}, the firing time $t_{fire} = n^{**} / RF_t$, and the projectile time of flight to the EDT t_{flight}

$$t^* = t_{prep\_fire} + t_{fire} + t_{flight}. \tag{4.26}$$

This time shall not exceed the duration of the window of enhanced danger Δt_{WED}

$$t^* < \Delta t_{WED}. \tag{4.27}$$

If condition (4.27) is not satisfied, the execution of the mission is considered impractical.

The safety of the artillery system is associated with the possibility of its detection by enemy artillery covering the EDT. It is assumed that detection occurs after four

shots [22]. In this case, the time of possible engagement of the artillery system is determined by the following expression

$$t_{fire}^{enemy} = 4 / RF_t + t_{prep}^{enemy} + t_{flight}, \tag{4.28}$$

where t_{fire}^{enemy} – the time required by the enemy to determine the coordinates of the TFP and prepare for firing. It is assumed here that the enemy covering artillery is deployed close to the EDT; therefore, the projectile time of flight is approximately the same as that from the TFP to the EDT.

If $t_{fire} + t_{flight} < t_{fire}^{enemy}$, the mission can be accomplished even under the risk of losing the artillery system, which is justified by the higher value of the EDT. If $t_{fire} + t_{flight} > t_{fire}^{enemy}$, the maneuverability criterion becomes decisive, and the artillery system must immediately leave the TFP.

4.7.4 Example of calculation and analysis of results

The effectiveness of the SPAS in engaging the EDT is evaluated under the condition of achieving the specified probability of destruction $p^* = 0.95$. The duration of the window of enhanced danger is $\Delta t_{WED} = 300$ s. The projectile time of flight is $t_{flight} = 60$ s; an analogous value is assumed for the projectiles of the enemy's covering artillery.

According to the results of the dynamic assessment, the SPAS is in the state $State^t <1,1.1;\ 2,2.1;\ 3,3.1;\ 4,4.1;\ 5,5.1>$, which corresponds to the "ideal point". The probability of a hit with a single shot is $p = 0.9$. According to (4.25), to ensure $p^* = 0.95$, $n^{**} = 4$ shots are required. Firing is conducted in the MRSI mode; the firing time is $t_{fire} = 30$ s, and the preparation time before opening fire is $t_{prep\_fire} = 20$ s.

The total time required to accomplish the mission is

$$t^* = t_{prep\_fire} + t_{fire} + t_{flight} = 20 + 30 + 60 = 110 \text{ s},$$

$110 \text{ s} < \Delta t_{WED} = 300$ s – therefore, the mission can be accomplished.

If detection occurs after the fourth shot during the 60 s projectile flight time, the system, moving at a speed of 60 km/h, relocates approximately 1 km from the TFP, thereby avoiding engagement.

The calculation results for different technical states of the system are summarized in **Table 4.2**, which makes it possible to compare the impact of system degradation on the required number of shots, mission duration, and final outcome.

Table 4.2 Comparative results of evaluating the SPAS effectiveness for different technical states

Example No.	State of the SPAS	p	n^{**}	t_{fire}, s	t^*, s	Result
1	Ideal	0.9	4	30	110	Mission without losses
2	Partial degradation	0.7	7	70	150	Mission with risk
3	Significant degradation	0.5	10	120	200	Mission with SPAS loss

Analysis of the tabulated data confirms a regular increase in mission execution time and in the required number of shots as the technical condition of the SPAS deteriorates, which increases the risk of its destruction.

The presented examples demonstrate the implementation of the four-component model of combat operations of the SPAS (**Fig. 4.11**).

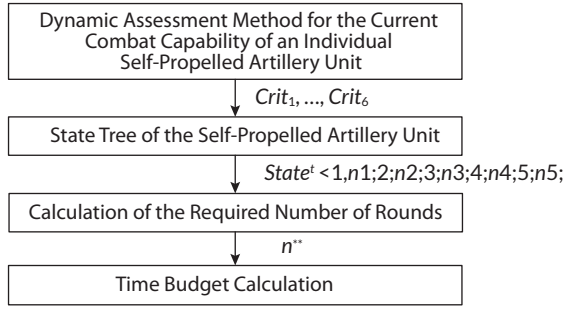

Fig. 4.11 Four-component model of combat operations of an individual SPAS

The obtained results are consistent with previously reported studies on acoustic identification of artillery shots and barrel wear modeling [15–19]. In contrast to earlier approaches focused on individual subsystems, the proposed method integrates acoustic, visual, thermodynamic, and mechanical parameters into a unified decision-support framework.

4.8 Conclusions

This chapter develops a comprehensive model for assessing the state of an artillery system as a multifactor dynamic object operating under conditions of accumulated wear and external combat impact. The integration of acoustic, visual, thermodynamic,

and mechanical parameters into a unified system for quantitative evaluation of technical condition and residual service life is substantiated. A state tree of the system is constructed, formalizing possible technical configurations of the SPAS and enabling a rank-based assessment of its combat capabilities. An analytical expression is derived for determining the required number of shots to engage a target with a specified probability, establishing a link between the system state and mission parameters.

A model for temporal evaluation of combat mission execution is proposed, taking into account the balance between firing time, maneuvering time, and the target engagement time window. An integrated system of combat capability criteria is developed with aggregation of indicators using the ideal point method, ensuring justified decision-making regarding the feasibility of opening fire.

The obtained results form a methodological basis for further automation of artillery system condition monitoring and may be implemented as an algorithmic module in decision support systems for combat employment.

Conflict of interest

The authors declare that they have no conflict of interest in relation to this research, whether financial, personal, authorship or otherwise, that could affect the research and its results presented in this paper.

Use of artificial intelligence statement

Artificial intelligence technology was used in the preparation of this chapter. Specifically, the authors used OpenAI ChatGPT (model GPT-5.2) to assist in editing and structuring introductory text sections and in formulating generalized descriptions of research methodologies for integrating mandatory literature sources into the chapter introduction.

The authors bear full responsibility for the final manuscript. Generative AI tools are not credited and are not responsible for the final results.

Authors' contributions

Oksana Maksymova: Conceptualization, Methodology, Development of integrated system model, Supervision, Writing – original draft.

Pavlo Gultsov: Literature review, Data curation, Comparative analysis, Writing – review & editing.

Volodymyr Demydenko: Mathematical modeling, Numerical analysis, Model validation, Visualization.

Yevhenii Dobrynin: Formal analysis, Development of evaluation criteria, Interpretation of results, Writing – review & editing.

References

1. Boltenkov, V., Brunetkin, O., Dobrynin, Y., Maksymova, O., Kuzmenko, V., Gultsov, P. et al. (2021). Devising a method for improving the efficiency of artillery shooting based on the Markov model. Eastern-European Journal of Enterprise Technologies, 6 (3 (114)), 6–17. https://doi.org/10.15587/1729-4061.2021.245854
2. Dobrynin, Y., Volkov, V., Maksymov, M., Boltenkov, V. (2020). Development of physical models for the formation of acoustic waves at artillery shots and study of the possibility of separate registration of waves of various types. Eastern-European Journal of Enterprise Technologies, 4 (5 (106)), 6–15. https://doi.org/10.15587/1729-4061.2020.209847
3. Dobrynin, Y., Brunetkin, O., Maksymov, M., Maksymov, O. (2020). Constructing a method for solving the riccati equations to describe objects parameters in an analytical form. Eastern-European Journal of Enterprise Technologies, 3 (4 (105)), 20–26. https://doi.org/10.15587/1729-4061.2020.205107
4. Brunetkin, O., Beglov, K., Brunetkin, V., Maksymov, O., Maksymova, O., Havaliukh, O. et al. (2020). Construction of a method for representing an approximation model of an object as a set of linear differential models. Eastern-European Journal of Enterprise Technologies, 6 (2 (108)), 66–73. https://doi.org/10.15587/1729-4061.2020.220326
5. Brunetkin, O., Maksymov, M., Brunetkin, V., Maksymov, O., Dobrynin, Y., Kuzmenko, V. et al. (2021). Development of the model and the method for determining the influence of the temperature of gunpowder gases in the gun barrel for explaining visualize of free carbon at shot. Eastern-European Journal of Enterprise Technologies, 4 (1 (112)), 41–53. https://doi.org/10.15587/1729-4061.2021.239150
6. Brunetkin, O., Maksymov, M., Dobrynin, Y., Demydenko, V., Sidelnykov, O. (2024). Development of a process model for determining the composition and energy characteristics of a pyrotechnic mixture using the library method.

EUREKA: Physics and Engineering, 5, 99–112. https://doi.org/10.21303/2461-4262.2024.003453
7. Brunetkin, O., Dobrynin, Y., Maksymenko, A., Maksymova, O., Alyokhina, S. (2020). Inverse problem of the composition determination of combustion products for gaseous hydrocarbon fuel. Computational Thermal Sciences: An International Journal, 12 (6), 477–489. https://doi.org/10.1615/computthermalscien.2020034878
8. Maksymov, M. V., Brunetkin, O. I., Beglov, K. V., Alyokhina, S. V., Butenko, O. V. (2022). Automatic Control for the Slow Pyrolysis of Organic Materials with Variable Composition. Advanced Control Systems. River Publishers, 397–434. https://doi.org/10.1201/9781003337010-16
9. Brunetkin, O. I., Beglov, K. V., Maksymov, M. M., Ulytska, O. O. (2021). Model and method of controlled pyrolysis of organic substances ofvariable composition. International Scientific Technical Journal "Problems of Control and Informatics", 66 (1), 134–146. https://doi.org/10.34229/1028-0979-2021-1-12
10. Brunetkin, O., Sidelnykov, O., Maksymov, M., Dobrynin, Y. (2025). Improving the model for determining the composition of gunpowder gases during thermal destruction of gunpowder in a limited volume space. Eastern-European Journal of Enterprise Technologies, 3 (6 (135)), 35–45. https://doi.org/10.15587/1729-4061.2025.330654
11. Miller, S. W. (2017). Shoot and scoot. Armada International. Available at: https://www.armadainternational.com/2017/08/shoot-scoot-artillery/
12. Nadler, J., Eilbott, J. (1971). Optimal Sequential Aim Corrections for Attacking a Stationary Point Target. Operations Research, 19 (3), 685–697. https://doi.org/10.1287/opre.19.3.685
13. Shim, Y., Atkinson, M. P. (2018). Analysis of artillery shoot-and-scoot tactics. Naval Research Logistics (NRL), 65 (3), 242–274. https://doi.org/10.1002/nav.21803
14. Guzik D. M. (1988). Markov model for measuring artillery fire support effectiveness [Master's thesis; Naval Postgraduate School].
15. Akman, Ç. (2017). Multishooter localization with acoustic sensors [Master's thesis; Middle East Technical University].
16. Brunetkin, O., Kuzmenko, V., Soloviova, O. (2022). Mathematical model of energy transformation processes in barrel system for determining shooting performance. Energy Engineering and Control Systems, 8 (1), 28–39. https://doi.org/10.23939/jeecs2022.01.028
17. Dobrynin, Y. V., Boltenkov, V. O., Kuzmenko, V. V., Maksymov, O. M. (2022). Development of a universal binary classifier of the state of artillery barrels by

the physical fields of shots. Applied Aspects of Information Technology, 5 (4), 289–302. https://doi.org/10.15276/aait.05.2022.19
18. Maksymov, M. V., Kuzmenko, V. V., Soloviova, O. V. (2021). Method for determining the temperature of powder gases along the barrel length during the firing process. Results of Modern Scientific Research and Development. Proceedings of the 7th International Scientific and Practical Conference. Madrid: Barca Academy Publishing, 95–99. Available at: https://sci-conf.com.ua/vii-mezhdunarodnaya-nauchno-prakticheskaya-konferentsiya-results-of-modern-scientific-research-and-development-19-21-sentyabrya-2021-goda-madrid-ispaniya-arhiv/
19. Tarakhtii, O. S., Kuzmenko, V. V. (2022). Avtomatyzovane diahnostuvannia postriliv artyleriiskoi harmaty na osnovi parametriv, yaki maiut riznu fizychnu pryrodu vynyknennia. Eurasian Scientific Discussions. Proceedings of the 10th International Scientific and Practical Conference. Barcelona: Barca Academy Publishing, 149–156. Available at: https://sci-conf.com.ua/wp-content/uploads/2022/10/EURASIAN-SCIENTIFIC-DISCUSSIONS-23-25.10.22.pdf
20. ARCHER Mobile Howitzer. BAE Systems. Available at: https://www.baesystems.com/en/product/archer
21. Horbenko, V., Kuchynska, A., Hudym, V. (2023). Features of targeting in current combined and future multi-domain operations. Air Power of Ukraine, 2 (5), 10–16. https://doi.org/10.33099/2786-7714-2023-2-5-10-16
22. Kopp, C. (2005). Artillery for the army: Precision fire with mobility. Defence Today, 4 (3), 12–16. Available at: https://www.ausairpower.net/SP/DT-SPH-0705.p